Induction of Nonbilayer Structures in Diacylphosphatidylcholine Model Membranes by Transmembrane α-Helical Peptides: Importance of Hydrophobic Mismatch and Proposed Role of Tryptophans†

J. Antoinette Killian,*,‡ Irene Salemink,‡ Maurits R. R. de Planque,‡ Göran Lindblom,§ Roger E. Koeppe II,|| and Denise V. Greathouse||

Department Biochemistry of Membranes, Center for Biomembranes and Lipid Enzymology, Institute of Biomembranes, Utrecht University, Padualaan 8, 3584 CH Utrecht, The Netherlands, Department of Physical Chemistry, University of Umeå, Umeå, Sweden, and Department of Chemistry and Biochemistry, University of Arkansas, Fayetteville, Arkansas 72701

Received August 25, 1995; Revised Manuscript Received November 7, 1995⊗

ABSTRACT: We have investigated the effect of several hydrophobic polypeptides on the phase behavior of diacylphosphatidylcholines with different acyl chain length. The polypeptides are uncharged and consist of a sequence with variable length of alternating leucine and alanine, flanked on both sides by two tryptophans, and with the N- and C-termini blocked. First it was demonstrated by circular dichroism measurements that these peptides adopt an α-helical conformation with a transmembrane orientation in bilayers of dimyristoylphosphatidylcholine. Subsequent ^{31}P NMR measurements showed that the peptides can affect lipid organization depending on the difference in hydrophobic length between the peptide and the lipid bilayer in the liquid-crystalline phase. When a 17 amino acid residue long peptide (WALP17) was incorporated in a 1/10 molar ratio of peptide to lipid, a bilayer was maintained in saturated phospholipids containing acyl chains of 12 and 14 C atoms, an isotropic phase was formed at 16 C atoms, and an inverted hexagonal (H_{II}) phase at 18 and 20 C atoms. For a 19 amino acid residue long peptide (WALP19) similar changes in lipid phase behavior were observed, but at acyl chain lengths of 2 C-atoms longer. Also in several cis-unsaturated phosphatidylcholine model membranes it was found that these peptides and a shorter analog (WALP16) induce the formation of nonbilayer structures as a consequence of hydrophobic mismatch. It is proposed that this unique ability of the peptides to induce nonbilayer structures in phosphatidylcholine model membranes is due to the presence of two tryptophans at both sides of the membrane/water interface, which prevent the peptide from aggregating when the mismatch is increased. Comparison of the hydrophobic length of the bilayers with the length of the different peptides showed that it is the precise extent of mismatch that determines whether the preferred lipid organization is a bilayer, isotropic phase, or H_{II} phase. The peptide-containing bilayer and H_{II} phase were further characterized after sucrose density gradient centrifugation of mixtures of WALP16 and dioleoylphosphatidylcholine. ^{31}P NMR measurements of the isolated fractions showed that a complete separation of both components was obtained. Chemical analysis of these fractions in samples with varying peptide concentration indicated that the H_{II} phase is highly enriched in peptide (peptide/lipid molar ratio of 1/6), while the maximum solubility of the peptide in the lipid bilayer is about 1/24 (peptide/lipid, molar). A molecular model of the peptide-induced H_{II} phase is presented that is consistent with the results obtained thus far.

In recent years it has become increasingly clear that the extent of hydrophobic matching between proteins and lipids in membranes can play an important role in membrane structure, function, and biogenesis. Hydrophobic mismatch could be responsible for processes like lateral segregation of proteins in biological membranes and the formation of lipid microdomains (Sperotto & Mouritsen, 1993; Marsh, 1995). It may be a key factor in controlling protein function and assembly, as suggested by reconstitution studies of membrane proteins in lipid bilayers of varying thickness (Montecucco et al., 1982; Riegler & Möhwald, 1986; Lewis & Engelman, 1983a). An important role for hydrophobic (mis)matching is furthermore suggested by the observed correlation between the length of the membrane-spanning part of proteins in different biological membranes and the hydrophobic thickness of these membranes (Bretscher & Munro, 1993; Pelham & Munro, 1993).

A rationale for the potential importance of hydrophobic (mis)match is the following. If the hydrophobic part of a protein would be either too short or too long to span the membrane, this would result in exposure of hydrophobic surfaces to an aqueous environment. To prevent this, the membrane can react in a number of ways, depending on the extent of mismatch and the nature of the proteins and lipids involved. Proteins could aggregate, tilt to change their effective hydrophobic length, slightly adapt their secondary structure, or adopt another conformation. The lipids can react by either stretching or disordering their hydrocarbon chains

† This work was supported in part by NIH Grant GM 34968 (to R.E.K. and D.V.G.), by a grant from the Swedish Natural Science Research Council to J.A.K., and by NATO grant CRG 950357.

* Corresponding author. Telephone: 31-30-2533442. Fax: 31-30-2522478. E-mail: killian@chem.ruu.nl.

‡ Utrecht University.

§ University of Umeå.

|| University of Arkansas.

⊗ Abstract published in *Advance ACS Abstracts,* December 15, 1995.

Table 1. Amino Acid Sequence of the Various Peptides Used and their Calculated Length, When Present as an α-Helix[a]

peptide	sequence	length (Å)
WALP16	HCO-AWWALALALALALWWA-$NHCH_2CH_2OH$	25.5
WALP17	HCO-AWWLALALALALALWWA-$NHCH_2CH_2OH$	27.0
WALP19	HCO-AWWLALALALALALALWWA-$NHCH_2CH_2OH$	30.0

[a] It is assumed that each amino acid has a length of 1.5 Å, with the C-terminal ethanolamine included as the length of an additional amino acid.

(Mouritsen & Bloom, 1984) or, more rigorously, by adopting a nonbilayer phase (Van Echteld et al., 1982; Killian et al., 1989). When mixtures of lipids are present, the protein may become surrounded preferentially by the lipids with the most optimal hydrophobic matching (Sperotto & Mouritsen, 1993; Zhang et al., 1992; Piknova et al., 1993).

Each of these rearrangements will have consequences for membrane structure and function. To investigate these consequences at a molecular level and to gain insight into the properties of proteins and lipids that determine what the consequences of hydrophobic mismatch will be in a particular system, it is necessary to carry out systematic studies on well-defined protein−lipid complexes. Since proteins are rather complex for such a study, a number of groups have taken the approach of using model peptides (Davis et al., 1982; Pauls et al., 1985; Roux et al., 1989; Zhang et al., 1992, 1995a,b; Watnick et al., 1990; Xing & Scott, 1992; Van Echteld et al., 1982; Killian et al., 1989; Greathouse et al., 1994; Deber & Li, 1995). One such model peptide is the hydrophobic, channel-forming pentadecapeptide gramicidin. In its channel conformation the peptide spans the membrane as a $\beta^{6.3}$-helical dimer in which the N-termini are linked together by hydrogen-bonding (Urry et al., 1971; Andersen et al., 1992; Killian, 1992).

When incorporated in phosphatidylcholine (PC) bilayers at high peptide/lipid molar ratios, gramicidin was shown to respond to a hydrophobic mismatch by inducing the formation of nonbilayer structures (Van Echteld et al., 1982; Killian et al., 1989). Such an effect on lipid organization is intriguing from the general point of view of membrane functioning, since nonbilayer structures have been implicated in a number of functional membrane processes (De Kruijff, 1987; Lindblom & Rilfors, 1992). However, the effect appears to be unique for gramicidin, since up until now it has not been observed for any other hydrophobic peptide in PC systems. This suggests that special properties of the gramicidin molecule are responsible for the induction of nonbilayer structures. Possible candidates are its unusual conformation, the ability of the gramicidin channel to dissociate, or the presence of four tryptophans near the lipid/water interface of each monomer [for review, see Killian (1992)].

In order to determine whether also α-helical peptides can induce the formation of nonbilayer structures, and to gain more general insight into the factors that determine the consequences of hydrophobic mismatch, we designed the WALP peptides, as shown in Table 1. These peptides have a hydrophobic core of alanine and leucine, both with a high propensity to form α-helical structures. When present as an α-helix, WALP16 and WALP17 are calculated to have approximately the same total length as the gramicidin channel (26 Å; Arseniev et al., 1986). The peptides furthermore resemble the gramicidin channel in that they are uncharged, have their N- and C-termini blocked, and are flanked on both sides with tryptophans. Because the tryptophans could be important for the interaction of these peptides with the lipids, their number and position near the interface were kept constant for investigation of length effects. It should be noted here that tryptophans and other aromatic amino acids are frequently found near the lipid/water interface in type I single membrane-spanning proteins (Landolt-Marticorena et al., 1993) as well as in multi-membrane-spanning proteins (Henderson et al., 1990; Weiss et al., 1991; Michel & Deisenhofer, 1990). The peptides therefore may also resemble a consensus sequence for a transmembrane α-helical segment of intrinsic membrane proteins.

In this study we focus on the effect of hydrophobic mismatch on lipid organization of diacylphosphatidylcholines with varying length and unsaturation, using the peptides shown in Table 1. We will demonstrate by circular dichroism that these peptides indeed adopt an α-helical conformation with a transmembrane orientation. Using ^{31}P NMR it will be shown that, like gramicidin, at high peptide/lipid ratios the peptides can induce nonbilayer structures in phosphatidylcholine model membranes, depending on the extent of mismatch. The results will be discussed in terms of hydrophobic mismatch and structural requirements of peptides to induce nonbilayer structures and prevent peptide aggregation.

MATERIALS AND METHODS

Materials

Fmoc-amino acids[1] and Fmoc-L-Ala resin were purchased from Advanced Chemtech (Louisville, KY). Boc-L-Ala resin was from Bachem Bioscience Inc. (Philadelphia, PA). Piperidine, 1.0 M 1-hydroxybenzotriazole (HOBT) in *N*-methylpyrrolidinone (NMP), and dicyclohexylcarbodiimide (DCC) in NMP were from Applied Biosystems, Inc. (Foster City, CA). NMP and methanol, Burdick and Jackson HPLC grade, and hexafluoro-2-propanol (HFIP), 99% Baker Analyzed, were purchased from Baxter Scientific (McGaw Park, IL). The HFIP was purified by distillation. Ethanolamine, from Aldrich Chemical Co. (Milwaukee, WI), was purified by vacuum distillation and stored in sealed ampules at 4 °C until use. Trifluoroacetic acid (TFA) was from Merck (Darmstadt, Germany) and 2,2,2-trifluoroethanol (TFE) from Sigma (St. Louis, MO). The phospholipids dimyristoylphosphatidylcholine (di-C14:0-PC), dipalmitoylphosphatidylcholine (di-C16:0-PC), distearoylphosphatidylcholine (di-C18:0-PC), diarachidoylphosphatidylcholine (di-C20:0-PC), dipalmitoleoylphosphatidylcholine (di-C16:1_c-PC), dioleoylphosphatidylcholine (di-C18:1_c-PC), and dierucoylphosphatidylcholine (di-C22:1_c-PC) were obtained from Avanti Polar

[1] Abbreviations: Aib, aminoisobutyric acid; Boc, *tert*-butyloxycarbonyl; CSA, chemical shift anisotropy; DCC, dicyclohexylcarbodiimide; DMF, dimethylformamide; Fmoc, 9-fluorenylmethoxycarbonyl; HFIP, hexafluoro-2-propanol; HOBT, 1-hydroxybenzotriazole; OMe, methoxy; NMP, *N*-methylpyrrolidinone; TFA, trifluoroacetic acid; TFE, trifluoroethanol.

Lipids Inc. (Birmingham, AL). The peptides WALP16, WALP17, and WALP19 were synthesized as described below.

Methods

Synthesis of WALP Peptides. Peptides were synthesized by Fmoc chemistry on an Applied Biosystems Model 431 peptide synthesizer. Fmoc-L-Ala resin was deprotected with 20% piperidine in NMP. Alternatively, as a test, a linkage that was stable to TFA was created by using a Boc-L-Ala resin, which was deprotected with 60% TFA in dichloromethane and then neutralized with 10% diisopropylethylamine. Fmoc amino acids were coupled as the HOBT-esters and also were deprotected with 20% piperidine in NMP. Each synthesis was completed by coupling previously prepared and recrystallized (Weiss & Koeppe, 1985) formyl-L-Ala, also as the HOBT-ester.

The peptide/resins were dried under vacuum (<0.005 mm Hg) for 24 h, and the peptides were cleaved from the resins using 50% distilled ethanolamine in either dimethylformamide (DMF) or distilled HFIP at 55 °C for 18 h. When DMF was the cosolvent, the peptides remained insoluble and could only be removed from the resins by a brief rinse with neat TFA. Following evaporation of the TFA, the peptides could be dissolved in TFE. Equivalent results for ethanolamine/DMF cleavage were obtained starting from either the Fmoc of the Boc-L-Ala resin. When HFIP was the cosolvent, the peptides were soluble and were removed from the resins by extensive rinsing with HFIP and TFE.

For each crude peptide in TFE and/or HFIP all except approximately 5 mL of filtrate was removed by rotary evaporation. The remaining filtrates were precipitated with 4 volumes of deionized H_2O and were left at 4 °C for at least 30 min. The precipitated solutions were centrifuged at 4 °C for 2 h at 20 400*g*. The supernatants were discarded, the pellets were resuspended in 5 mL of TFE, and the precipitation and centrifugation steps were repeated. The pellets were dried to powder under vacuum.

The peptides were analyzed by electrospray mass spectroscopy (Mass Consortium Corp., San Diego, CA) and sequence analysis (Applied Biosystems 473A Protein Sequencer, Foster City, CA). Both mass spectroscopy and sequence analysis revealed that some desformyl peptide was present. The remaining peptide (80% or more) had the correct formyl−peptide−ethanolamine sequence and the corresponding molecular weight. The desformyl component could be removed by ion-exchange chromatography on the H^+ form of AGMP-50 (Bio-Rad Laboratories, Hercules, CA), with "flow-through" of the *N*-formyl peptides (Weiss & Koeppe, 1985). Equivalent results were obtained whether or not the minor desformyl component was removed.

Procedure for Peptide Incorporation. Phospholipid dispersions were prepared from chloroform solutions by drying off the solvent on a rotavapor, followed by storage overnight under high vacuum. The lipids were then dispersed in 0.5 mL of freshly distilled water at temperatures above the gel to liquid crystalline phase transition. Peptides were first dissolved in a small volume of TFA (10 μL per mg of peptide) and dried under a stream of nitrogen. Next, most of the residual TFA was removed by dissolving the peptide in 5 mL of TFE followed by evaporation of the solvent on a rotavapor. The peptide film was then dissolved in 0.5 mL of TFE and immediately was added, while vortexing, to the phospholipid dispersion, again at temperatures above the gel to liquid phase transition temperature. Next, water was added to yield a 16:1 ratio of water to TFE by volume. The samples were mixed by vortexing for 2 s and lyophilized after rapid freezing in CO_2/acetone by drying overnight under a vacuum of 0.05 mm Hg at −80 °C. Further sample handling was dependent on the type of measurement and is described along with those measurements.

^{31}P NMR Measurements. For NMR measurements lyophilized samples containing 20 μmol of lipid and a variable amount of peptide were rehydrated with similar results either in 1 mL of water or in buffer (100 mM NaCl, 25 mM Tris, pH 7.4). The samples were spun down at 30000*g* for 10 min at 4 °C, and the supernatant was removed. To remove residual TFE, the pellet was again dispersed in 1 mL of H_2O or buffer, and the procedure was repeated. ^{31}P NMR spectra of the pellets were recorded at 121.5 MHz on a Bruker MSL 300 spectrometer, with a 17 μs 90° pulse, a 1.3 s interpulse time, and using gated proton-noise decoupling. A total of 1000−5000 free induction decays were accumulated. Prior to Fourier transformation an exponential multiplication was applied, resulting in a 100 Hz linebroadening. All spectra were scaled to the same height. The chemical shift anisotropy (CSA) of the bilayer or H_{II} phase components was determined as three times the distance between, respectively, the high field peak (bilayer) or the low field peak (H_{II} phase) and the isotropic position (position of DOPC sonicated vesicles). Percentages of nonbilayer structures were determined by computer substraction of pure bilayer spectra and integration of peak areas before and after substraction.

Circular Dichroism. For circular dichroism measurements lyophilized samples containing a variable amount of lipid and 0.25 μmol of peptide were rehydrated in 1 mL of water. To remove any residual TFE, the samples were pelleted down, the supernatant was removed, and the pellet was again dispersed in 1 mL of H_2O. Samples were then sonicated during 10 × 15 s with 60 s intervals and with an input power of 40 W, using a Branson 250 tip sonicator. To pellet down titanium particles and any residual multilamellar structures, the sonicated samples were next centrifuged for 20 min at 14 000 rpm in an Eppendorf centrifuge. The peptide concentration was measured after dilution of the sample in methanol by measuring the absorbance at 280 nm. A molar extinction coefficient ϵ of 21 300 M^{-1} cm^{-1} was used, calculated on weight basis. All sample handling was done at room temperature.

Circular dichroism (CD) measurements were carried out on a JASCO J-600 spectropolarimeter, using a 0.2 mm path length cell, 1 nm bandwidth, 0.1 nm resolution, 125 ms response time, and a scan speed of 50 nm/min. Spectra of all samples were baseline corrected by using control samples that were similarly prepared but in the absence of peptide. Oriented spectra were measured as described (De Jongh et al., 1994) after spreading 10 μL of a sonicated sample on a quartz plate, followed by air drying. Unless indicated otherwise all spectra were recorded at room temperature.

Sucrose Density Gradient Centrifugation. Samples first used for NMR measurements were dispersed in 1 mL of water and brought on top of a linear sucrose gradient (5.5 till 17.5%). The samples were centrifuged for 20 h at 150000*g* at 4 °C in a Beckman SW41 rotor. Separate bands were isolated and analyzed by ^{31}P NMR as described above.

Next, the peptide content was determined by UV absorbance at 280 nm, as described above, after dilution of the sample in methanol, and the lipid content was determined according to Rouser et al. (1970).

RESULTS

Incorporation of Peptides. The peptides used in this study are extremely hydrophobic and difficult to handle. They are insoluble in chloroform, but they can dissolve, after TFA treatment, in some other organic solvents, such as methanol, ethanol, trifluoroethanol, and hexafluoro-2-propanol (see Materials and Methods). However, in all of these solvents the peptides aggregate in time. Therefore, the conventional method of sample preparation by cosolubilizing peptide and lipid in organic solvent, followed by drying and hydration of the mixed peptide/lipid film, did not appear suitable as a general method to obtain homogeneous peptide/lipid dispersions. Hence, a new protocol was used, based on a method previously designed for incorporation of hydrophobic peptides into micelles (Killian et al., 1994). In short, the peptides are freshly dissolved in TFE, a good solvent for most hydrophobic peptides, but not a general solvent for lipids. The peptide solution is then immediately added to an equal volume of preformed lipid bilayers in water. The rationale is that the large amount of TFE will destabilize the bilayers and promote homogeneous association of the peptide with the lipids. Upon addition of excess water it then may be expected that stable bilayers are formed with the peptide incorporated. Next all solvent is removed by lyophilization, and the dry powder is rehydrated to form peptide/lipid dispersions. The advantage of this protocol is that it is independent of the solubility behavior of the peptide and the lipid. Control measurements using this protocol to prepare samples of gramicidin (which readily dissolves in many organic solvents) and different lipids gave essentially the same results as the "cosolubilization" method in terms of lipid phase behavior and effects on ^{31}P chemical shift anisotropy (see also below).

Conformation and Orientation of the Peptides in Lipid Bilayers. The above protocol was first used to prepare samples for investigation of the conformation and orientation of the peptides by CD (De Jongh et al., 1994). For these experiments di-C14:0-PC was chosen, because in this lipid a bilayer configuration is maintained (see below) in the presence of each peptide. Figure 1 (curve a) shows that when WALP17 is incorporated in sonicated vesicles of di-C14:0-PC, a spectrum is obtained with two minima near 222 and 208 nm, a cross-over at 202 nm, and a maximum near 192 nm, typical for an α-helical structure (Greenfield & Fasman, 1969). Similar spectra were obtained for WALP16 and WALP19 in di-C14:0-PC bilayers (data not shown). Also upon varying the peptide/lipid ratio in the range of 1/10 to 1/50 or upon varying the temperature in the range of 5−50 °C, no significant changes in lineshape were observed (not shown).

The WALP peptides are suitable to investigate the consequences of hydrophobic mismatch only if they adopt a transmembrane orientation. When peptide-containing lipid bilayers are oriented with their normal parallel to the incoming light, such a transmembrane orientation of the peptide would result in characteristic and well-defined CD spectra, in which the intensity of the absorption band near

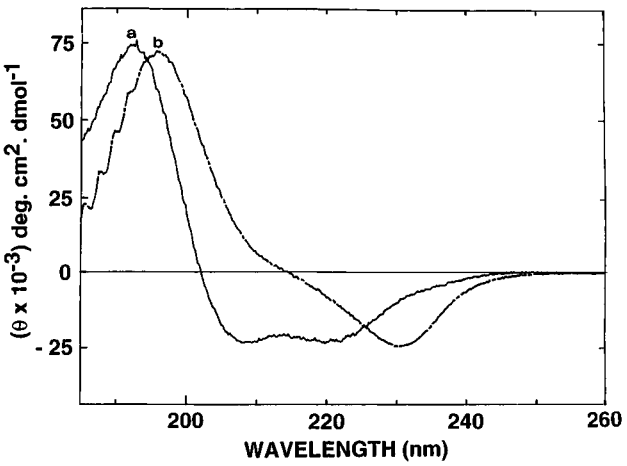

FIGURE 1: Circular dichroism spectra of WALP17 in di-C14:0-PC at a 1/25 ratio of peptide to lipid in (a) sonicated vesicles in excess water and (b) oriented bilayers. The ellipticity in spectrum b is not absolute, and scaled to that in spectrum a.

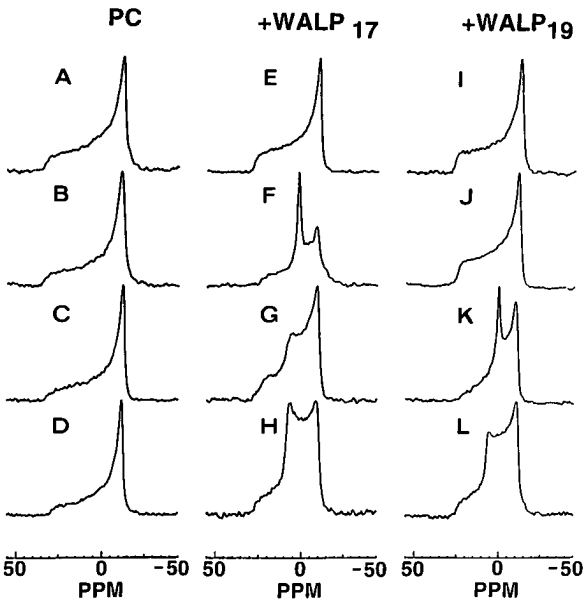

FIGURE 2: ^{31}P NMR spectra of dispersions of di-C14:0-PC (A, E, I), di-C16:0-PC (B, F, J), di-C18:0-PC (C, G, K), and di-C20:0-PC (D, H, L), in the absence (A−D) and presence of WALP17 (E−H) and WALP19 (I−L), in a molar ratio of peptide to lipid of 1/10 and at temperatures just above the gel to liquid-crystalline phase transition, of 25, 42, 56, and 70 °C, respectively.

208 nm is reduced to zero (De Jongh et al., 1994). Indeed, upon orienting the bilayers a spectrum was obtained (Figure 1, curve b) similar to that expected for α-helices oriented with their long axis parallel to the incoming light (De Jongh et al., 1994). Again, similar results were found for WALP16 and WALP19 (data not shown). Thus, it can be concluded that all three peptides form transmembrane α-helices, a first indication that the interfacially localized tryptophans can act as membrane anchors.

Effects on Lipid Phase Behavior in Saturated Lipids. The effect of the peptides on lipid phase behavior at high peptide/lipid ratios was investigated by ^{31}P NMR. Figure 2 shows ^{31}P NMR spectra of dispersions of saturated phosphatidylcholines in the absence and presence of WALP17 and WALP19 at a 1/10 molar ratio of peptide to lipid. For comparison all spectra were recorded just above the gel to liquid-crystalline phase transition temperature of the pure lipids (see Table 2). In the absence of peptide all lipids show

Table 2: Hydrophobic Thickness of the Various Phosphatidylcholine Bilayers in the Liquid-Crystalline Phase and the Gel to Liquid-Crystalline Phase Transition Temperatures of the Different Lipids

lipid	hydrophobic thickness (Å)	transition temperature (°C)
di-C14:0-PC	22.8[a]	24.0[c]
di-C16:0-PC	26.3[a]	41.5[c]
di-C18:0-PC	29.8[a]	54.3[c]
di-C20:0-PC	32.8[a]	64.1[c]
di-C16:1$_c$-PC	23.5[b]	−36[d]
di-C18:1$_c$-PC	27[b]	−14[d]
di-C22:1$_c$-PC	34[b]	11[e]

[a] Thicknesses calculated according to Sperotto and Mouritsen (1988). [b] From Lewis and Engelman (1983b). Values given by these authors for hydrophobic thicknesses in saturated lipids correspond well with those presented in this table. [c] From Blume (1983). [d] From Van Dijck et al. (1976). [e] From Caffrey and Feigenson (1981).

spectra with a low field shoulder and a high field peak, typical for a bilayer organization (Seelig, 1978; Cullis & De Kruijff, 1979). Upon incorporation of WALP17 in di-C14:0-PC, a bilayer organization is maintained, and the residual chemical shift anisotropy (CSA) decreases from 42 to 36 ppm. Together with the observation that the peaks are sharp and well-defined, this indicates that the peptides are homogeneously incorporated. In di-C16:0-PC an isotropic component is observed upon peptide incorporation, demonstrating destabilization of the lipid bilayer. This component could not be removed by centrifugation and therefore is not due to the presence of small vesicles. Most likely it can be attributed to the presence of a cubic phase, as often observed for lipids at positions in the phase diagram between a lamellar and reversed hexagonal (H_{II}) phase (Lindblom & Rilfors, 1989). Upon further increasing the acyl chain length to 18 C atoms, a second spectral component is observed with a low field peak near 5 ppm, superimposed on a bilayer component. This second component is typical for lipids in an inverted hexagonal (H_{II}) phase, which in a pure form shows a spectrum with an inverted asymmetry and a 2-fold reduced CSA as compared to the bilayer (Seelig, 1978; Cullis & De Kruijff, 1979). The relative amount of lipids present in the H_{II} phase increases with the acyl chain length, as evident from the higher intensity of the low field peak in di-C20:0-PC.

For WALP17 and 19, almost identical NMR spectra are obtained when the acyl chains for the latter are two carbon atoms longer. WALP19 in an α-helical conformation is calculated to be 3 Å longer than WALP17 and an increase by two methylenes in the acyl chains will result in an increase in bilayer thickness of about the same amount (see Table 2). Thus, it can be concluded that it is the extent of hydrophobic mismatch that is responsible for the effects of the peptides on lipid phase behavior. This would also imply that WALP17 and WALP19 adopt an orientation with the helix axis parallel to the lipid acyl chains, in line with the CD results.

Temperature and Concentration Dependence of Lipid Organization. A surprisingly large difference was observed in temperature dependence of the amount of isotropic phase and H_{II} phase of the different samples. Mixtures of WALP19 and di-C18:0-PC in a 1/10 molar ratio show a pure isotropic phase at 65 °C, as shown in Figure 3D, whereas at 56 °C only 16% of the lipids was found to undergo isotropic motion

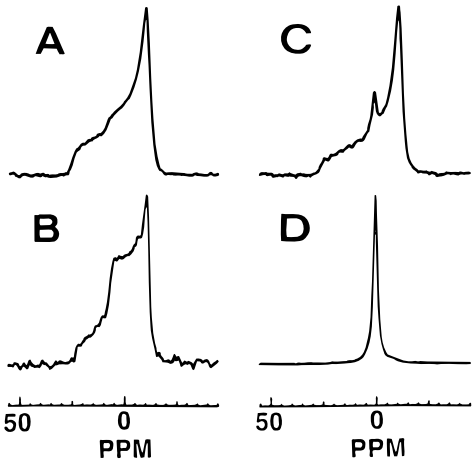

FIGURE 3: ^{31}P NMR spectra of dispersions of di-C18:0-PC in the presence of WALP17 (A and B) and WALP19 (C and D) in a molar ratio of peptide to lipid of 1/20 (A and C) and 1/10 (B and D) and at 65 °C.

(see Figure 2K). Similarly, in di-C16:0-PC in the presence of WALP17 a pure isotropic component was observed upon raising the temperature to 50 °C (not shown). In contrast, the relative intensity of the H_{II} phase characteristic component, induced by WALP17 in di-C18:0-PC, increases only slightly, from 16% to 24%, upon raising the temperature from 56 to 65 °C (compare Figure 3B with Figure 2G). These data suggest that the energy barrier for formation of an isotropic phase is relatively small. However, for the formation both of an isotropic phase and of an H_{II} phase, high concentrations of peptide are required. At a 1/20 molar ratio of peptide to lipid and at 65 °C only small amounts (5−6%) of either component are observed (Figure 3A,C). Thus, it can be concluded that the formation of the pure isotropic phase is a highly cooperative process. At a 1/30 molar ratio of peptide to lipid in all cases a pure bilayer spectrum was obtained (data not shown).

Effects on Phase Behavior of Unsaturated Lipids. The effect of the different WALP length analogs was also investigated upon incorporation in bilayers of unsaturated lipids with varying thickness. These measurements were done at 30 °C, at which temperature all the lipids are in the liquid-crystalline phase (see Table 2). Again a similar trend is observed. The ^{31}P NMR spectra of the pure lipids in Figure 4 show that these are organized in bilayers. When the shortest peptide (WALP16) is incorporated, an isotropic phase is induced in di-C16:1c-PC and an H_{II} phase in di-C18:1c-PC. For WALP17 an isotropic phase is induced in both di-C16:1c-PC and di-C18:1c-PC, suggesting that the small increase in length of WALP17 is sufficient to inhibit H_{II} phase formation in the latter lipid system. The longest peptide, WALP19, is unable to perturb the bilayer organization in di-C16:1c-PC but induces an isotropic phase in di-C18:1c-PC, similar to WALP17. In di-C22:1c-PC all three peptides are able to induce an H_{II} phase, with the relative amount of H_{II} phase increasing with the extent of hydrophobic mismatch.

Further Characterization of WALP-Induced H_{II} Phase Formation. To gain more insight into the mechanism of H_{II} phase formation at a molecular level, sucrose density gradient centrifugation measurements were carried out on a mixture of WALP16 and di-C18:1c-PC at a 1/10 molar ratio, which consists of about 63% bilayer and 37% H_{II} phase (see Figure

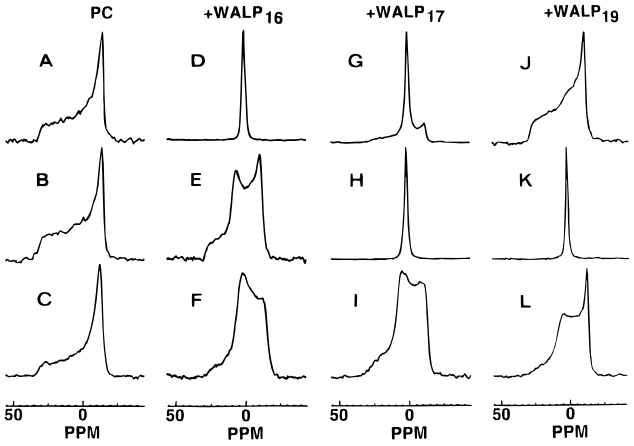

FIGURE 4: ^{31}P NMR spectra of dispersions of di-C16:1$_c$-PC (A, D, G, J), di-C18:1$_c$-PC (B, E, H, K), and di-C22:1$_c$-PC (C, F, I, L), in the absence (A−C) and presence of WALP16 (D−F), WALP17 (G−I) and WALP19 (J−L), in a molar ratio of peptide to lipid of 1/10 and at 30 °C.

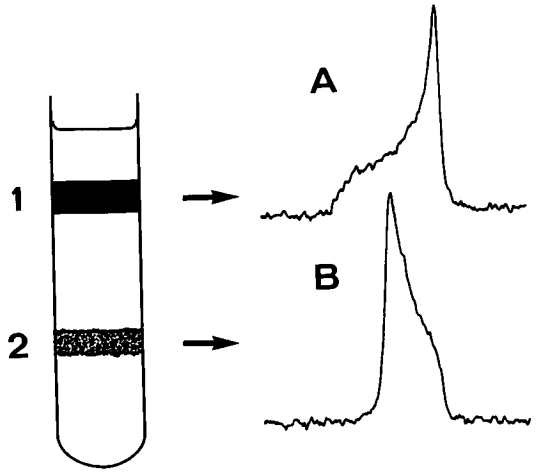

FIGURE 5: Illustration of the separation by sucrose density gradient centrifugation of a mixture of di-C18:1$_c$-PC and WALP16 (1/10, molar ratio of peptide to lipid) at 30 °C into two different components. One band occurs at a density of 1.058 g/mL (band 1), which, after isolation, gives a ^{31}P NMR spectrum typical for a bilayer organization of lipids (A). The other band occurs at a density of 1.126 g/mL (band 2) and gives a ^{31}P NMR spectrum typical for an H_{II} phase (B).

4E). The mixture was found to separate into two well defined bands at densities 1.058 and 1.126 g/mL. These bands were isolated and characterized by ^{31}P NMR, as shown in Figure 5. The line shape observed for the upper band corresponds to that of a pure bilayer, while the lower band gives a line shape typical for lipids organized in an H_{II} phase. Thus, the centrifugation experiments allow a complete separation of the bilayer and H_{II} phase component. Next the peptide and lipid content of the samples was analyzed. It was found that the peptide is highly enriched in the H_{II} phase, with a peptide/lipid ratio of 1/6, while in the bilayer a peptide/lipid ratio of 1/24 is observed.

^{31}P NMR spectra were then recorded of WALP16 and di-C18:1c-PC at different molar ratios, and for each sample the percentage H_{II} phase was determined. These values are plotted in Figure 6. The results clearly show that the percentage of H_{II} phase increases with the peptide concentration and that a minimum ratio of peptide to lipid is required that is larger than 1/30. These samples were next subjected to sucrose density gradient centrifugation. Interestingly, also

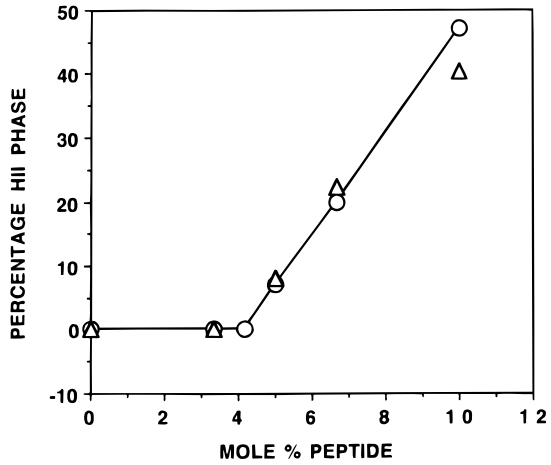

FIGURE 6: Percentage H_{II} phase in mixtures of WALP16 and di-C18:1$_c$-PC as calculated from ^{31}P NMR measurements (△) and as predicted on the basis of a two-phase coexistence of a bilayer with a peptide/lipid molar ratio of 1/24 and an H_{II} phase with a peptide/lipid molar ratio of 1/6 (○).

samples with initial peptide/lipid molar ratios of 1/15 and 1/20 were found to split into two bands with similar densities as in the sample with a 1/10 molar ratio. The lower bands in both cases had a peptide/lipid ratio of 1/6, while in the upper band the ratio varied from 1/24 to 1/26. This suggests that the peptide has a maximum solubility in the bilayer of approximately 1/24, after which a two-phase coexistence occurs, with well-defined bilayer and H_{II} phase components. Based on such a two-phase coexistence, the expected percentage H_{II} phase can be calculated in mixtures of WALP16 and di-C18:1c-PC at different ratios. As shown in Figure 6, these values correspond rather well with the experimentally observed values.

DISCUSSION

In this study we investigated the conformation, orientation, and effects on lipid phase behavior of a series of synthetic peptides in PC model membranes with varying thickness. The peptides were shown to form α-helices, as expected, because of their sequence of alternating Leu and Ala. CD on oriented bilayers furthermore demonstrated that the peptides adopt a transmembrane orientation, even though they contain no end charges to secure such an orientation. This indicates that the tryptophans, localized at both ends of these α-helical peptides, can act as membrane anchors.

Because of their transmembrane orientation, the WALP peptides are suitable as model peptides to investigate the influences of hydrophobic mismatch of peptides in lipid bilayers. These consequences will depend not only on the physicochemical properties of the peptides but also on those of the lipids. In this study we used model membranes of PC, which typically forms bilayers. Formation of an H_{II} phase in this lipid system is inhibited due to the relatively large size of the headgroup. However, upon incorporation of high amounts of the WALP peptides (10 mol %) it was found that nonbilayer structures are induced as a consequence of hydrophobic mismatch. Interestingly, the preferred nonbilayer phase, i.e., isotropic or H_{II}, appears to be strictly determined by the precise extent of mismatch. This is illustrated in Figure 7, where the difference between the length of a particular peptide and the hydrophobic length of the bilayer is given for each sample, along with the preferred

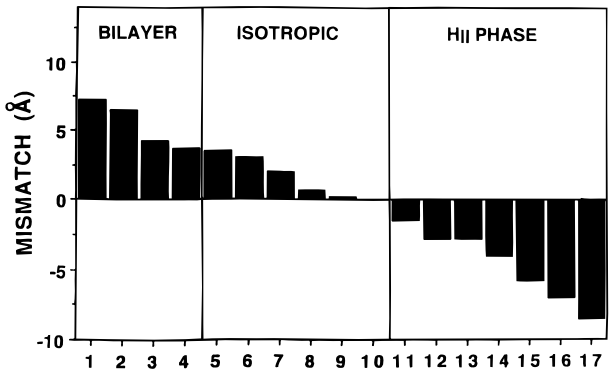

FIGURE 7: Phase preference as a function of mismatch. The mismatch in this Figure is defined as the difference between the length of the peptides, as given in Table 1, and the hydrophobic thickness of the lipid bilayers, as given in Table 2. Each bar represents one of the samples of which the ^{31}P NMR spectra are presented in Figures 2 and 4. (1) WALP19 + di-C14:0-PC, (2) WALP19 + di-C16:1c-PC, (3) WALP17 + di-C14:0-PC, (4) WALP19 + di-C16:0-PC, (5) WALP17 + di-C16:1c-PC, (6) WALP19 + di-C18:1c-PC, (7) WALP16 + di-C16:1c-PC, (8) WALP17 + di-C16:0-PC, (9) WALP19 + di-C18:0-PC, (10) WALP17 + di-C18:1c-PC, (11) WALP16 + di-C18:1c-PC, (12) WALP17 + di-C18:0-PC, (13) WALP19 + di-C20:0-PC, (14) WALP19 + di-C22:1c-PC, (15) WALP17 + di-C20:0-PC, (16) WALP17 + di-C22:1c-PC, (17) WALP16 + di-C22:1c-PC. The areas marked isotropic and H_{II} phase indicate spectra of which part or all of the lipids are present in an isotropic or H_{II} phase, respectively.

phase as concluded from the ^{31}P NMR measurements. The results suggest that an H_{II} phase is formed when the total length of the peptide is smaller than the hydrophobic thickness of the bilayer and an isotropic phase is formed when this length is slightly longer. In this latter case, the peptides are still expected to be much shorter than the distance between the phosphates on both sides of the lipid bilayer, which is about 11 Å more than the hydrophobic thickness (Lewis & Engelman, 1983b). When the total length of the peptide increases further, a stable bilayer is formed. The boundaries between isotropic phase and bilayer appear to be within a narrow region. The sample of WALP17 in the presence of di-C16:1c-PC (bar number 5 in Figure 7) may be very close to the borderline between a preference for a bilayer organization and an isotropic phase, because in this sample a small bilayer component is still present, while the other samples in this region (numbers 6−10) show a pure isotropic phase when the temperature is well above the liquid-crystalline phase transition temperature of the lipids.

How can these preferences for a particular phase be understood? Let us begin with the H_{II} phase. Figure 8 shows a model for the WALP-induced H_{II} phase in PC model membranes that is analogous to a model proposed previously for gramicidin (Killian, 1992) and that is consistent with all results so far. In this model the peptides each span the distance between two tubes. Since the peptide fills only the hydrophobic volume, the available area per head group will increase, relieving the steric constraints which normally will inhibit the formation of an H_{II} phase for phosphatidylcholine and allowing these lipids to organize in structures with highly curved interfaces. This would explain the requirement for a minimum mismatch, as suggested from Figure 7, as well as the requirement for such a high peptide/lipid ratio (1/6). Due to the decreased order of the acyl chains, the monolayer

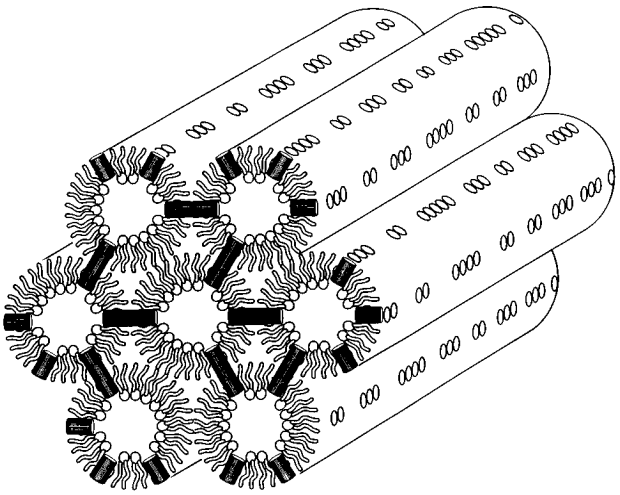

FIGURE 8: Model of the WALP-induced H_{II} phase. The peptides each span the distance between two tubes, such that all tryptophans are localized at the lipid/water interface. Since the peptides fill only the hydrophobic volume, the available area per head group will increase, relieving the steric constraints which normally will inhibit the formation of an H_{II} phase for phosphatidylcholine. Due to the increased disorder of the acyl chains, the monolayer thickness of a lipid in an H_{II} phase is much less than that of the same lipid in a bilayer. Hence, a peptide that is too short to fit into a bilayer will fit much better into an H_{II} phase formed by the same lipid.

thickness of a lipid in an H_{II} phase is much less than that of the same lipid in a bilayer. Hence, the peptide length, which is too small to fit in a bilayer, will match closely that of the hydrophobic thickness between adjacent tubes in the H_{II} phase.

The energy cost of H_{II} phase formation is among other factors determined by the requirement for the acyl chains to adapt to different lengths, depending on their position in the aggregate of the H_{II} phase at a particular time (Gruner, 1989; Sjölund et al., 1989). The monolayer thickness is smallest at the connections between adjacent water tubes, and the peptides are believed to be localized at exactly this position (Figure 5). Therefore, the mismatch may also reduce the energy cost of H_{II} phase formation.

Similar arguments may explain the induction of the isotropic structures that are observed with a smaller extent of mismatch. It is likely that these structures represent a cubic phase (e.g., a bicontinuous or a molten cubic phase; Lindblom & Rilfors, 1989), because (1) the position of cubic phases in the phase diagram is normally inbetween bilayer and inverted H_{II} phases, which is exactly where the isotropic signals are observed, and (2) the presence of small vesicles, which in principle could also give rise to isotropic NMR signals, can be excluded, since these structures would not have pelleted down with the rest of the sample during centrifugation. It then can be argued that also in a cubic phase the monolayer thickness will vary, although much less than in an H_{II} phase, and that the peptides may localize preferably at those sites where the thickness is minimal. However, the net curvature of a cubic phase will be much less than that of an H_{II} phase, and this is most likely the reason why the required mismatch is much smaller. The peptides can extend only a few angstroms above the hydrophobic part of the bilayer. If they extend too far (bar numbers 1−5 in Figure 7), formation of a cubic phase will not be favorable any longer: a bilayer organization will be maintained, even though the total length of the peptides is

still expected to be shorter than the phosphate to phosphate distance in the bilayer. In di-C16:0-PC an isotropic component is observed upon peptide incorporation, demonstrating destabilization of the lipid bilayer.

For the formation of both an H_{II} phase and an isotropic phase, relatively high concentrations of peptide were found to be required. It is not clear what the results of mismatch will be when insufficient peptide is available in the membrane to induce these phases. Possible consequences could be assembly of the peptides as oligomers, local adjustment of lipid chain order, and/or reorientation of the tryptophan residues to reduce the mismatch.

The formation of nonbilayer structures in PC bilayers by transmembrane peptides is a striking result, because up until now this behavior has not been observed for any other peptide, except for the channel forming peptide gramicidin A (Van Echteld et al., 1982; Killian et al., 1989). Even the uncharged, hydrophobic α-helical polypeptide Boc-(L-Ala-Aib-L-Ala-Aib-L-Ala)$_3$-OMe (where Aib = aminoisobutyric acid), called P15, which is slightly shorter than gramicidin, was found to be unable to affect lipid organization under the same conditions (Aranda et al., 1987).

We propose that the difference in behavior of gramicidin and the WALP peptides, on one hand, and P15, on the other, is due to the presence of interfacially localized tryptophans in the former peptides, and that it is these residues that are responsible for the induction of nonbilayer structures in PC systems as a consequence of hydrophobic mismatch. This may be understood on the basis of the observed preference of tryptophan residues for the lipid/water interface (Wimley & White, 1993). In general, when the hydrophobic part of a protein is much too short to fit into a lipid bilayer, this will result in protein aggregation (Mouritsen & Bloom, 1984; Marsh, 1995). Our hypothesis is that interfacially localized tryptophans may inhibit such aggregation. By organizing into nonbilayer structures, the favorable interaction of the tryptophans with the lipid/water interface can be optimally retained, while at the same time the hydrophobic mismatch is reduced or even completely removed.

The reason for the preference of tryptophans for a localization at the lipid/water interface is not known, but it may be related to the solubilization properties of tryptophan in lipid aggregates. Tryptophan is slightly polar and may be dissolved to some extent in water. Like many other aromatic ring molecules, it therefore prefers to be solubilized in the interfacial region of a lipid aggregate [White & Wimley, 1994; S. Persson, G. Lindblom, and J. A. Killian, to be published]. This is in line with previous investigations on benzene, which has a solubility of 19 mM in water, where it has been shown that benzene is located close to the polar head groups in surfactant micelles (Lindblom et al., 1973). For tryptophan an interfacial localization may be further promoted by other favorable interactions, such as electrostatic interactions with the dipole moment of the indole ring and hydrogen-bonding in the interfacial region.

An important role for tryptophans in peptide/lipid interactions was previously suggested on the basis of experiments with gramicidin. For this molecule it is the preference of the C-terminal localized tryptophans for a lipid/water interface that is believed to be responsible for the formation of the N−N dimeric channel conformation in a lipidic environment [see Killian (1992), O'Connell et al. (1990), Durkin et al. (1992), and Salom et al. (1995)]. The tryptophans also were found to be essential for gramicidin-induced H_{II} phase formation in PC model membranes, consistent with the model presented above. Modification of these residues by formylation resulted in a complete loss of the ability of gramicidin to induce H_{II} phase formation (Killian et al., 1985). Interestingly, preliminary experiments with the WALP peptides indicated a similar loss of the ability to induce nonbilayer structures upon formylation of the tryptophan residues, supporting our suggestion that these residues play an important role in determining the consequences of hydrophobic mismatch for lipid organization.

Summarizing, we have shown that transmembrane α-helical peptides can induce nonbilayer structures as a consequence of hydrophobic mismatch in PC bilayers and that the nature of these nonbilayer structures depends on the precise extent of mismatch. We propose that the tryptophan residues, because of their preference for a lipid/water interface, are crucial for these effects of hydrophobic mismatch on lipid organization. Also for membrane proteins in general, tryptophan residues may have an important functional role, as suggested by their frequent occurrence near the lipid/water interface in many membrane proteins (Landolt-Marticorena et al., 1993; Henderson et al., 1990; Weiss et al., 1991; Michel & Deisenhofer, 1990; Haltia & Freire, 1995). It has been proposed that these tryptophans and other aromatic amino acids may serve as membrane anchors (Schultz, 1994). The present study not only supports such a role but suggests an additional functional role with implications for protein assembly: the preference of the tryptophans for a lipid/water interface may be important in determining the side to side packing of helices in a multimembrane-spanning protein, i.e., the helices may have a tendency to associate with the tryptophan containing sides away from each other and directed toward the lipids.

To further pin down the role of interfacially localized tryptophans for protein/lipid interactions, we will next investigate the effects on lipid structure of WALP analogs in which the number of tryptophans and their positions are varied and in which the tryptophans are substituted by other aromatic amino acids.

ACKNOWLEDGMENT

We thank Dr. B. de Kruijff for helpful suggestions on the manuscript and Philip Banda from Applied Biosystems, division of Perkin Elmer, Foster City, CA, for helpful suggestions regarding peptide synthesis.

REFERENCES

Andersen, O. S., & Koeppe, R. E., II (1992) *Physiol. Rev.* 72, S89−S158.
Aranda, F. J., Killian, J. A., & De Kruijff, B. (1987) *Biochim. Biophys. Acta 901*, 217−228.
Arseniev, A. S., Lomize, A. L., Barsukov, I. L., & Bystrov, V. F. (1986) *Biol. Membr. 3*, 1077−1104.
Blume, A. (1983) *Biochemistry 22*, 5436−5442.
Bretscher, M. S., & Munro, S. (1993) *Science 261*, 1280−128.
Caffrey, M., & Feigenson, G. W. (1981) *Biochemistry 20*, 1949−1961.
Chupin, V., Killian, J. A., & De Kruijff, B. (1987) *Biophys. J. 51*, 395−405.
Cullis, P. R., & De Kruijff, B. (1979) *Biochim. Biophys. Acta 559*, 399−420.
Davis, J. H., Hodges, R. S., & Bloom, M. (1982) *Biophys. J. 37*, 170−171.
Deber, C. M., & Li, S.-C. (1995) *Biopolymers 37*, 295−318.

De Jongh, H. H. J., Goormaghtigh, E., & Killian, J. A. (1994) *Biochemistry 33*, 14521−14528.
De Kruijff, B. (1987) *Nature 329*, 587−588.
Durkin, J. T., Providence, L. L., Koeppe, R. E., II & Andersen, O. S. (1992) *Biophys. J. 62*, 145−149.
Greathouse, D. V., Hinton, J. F., Kim, K. S., & Koeppe, R. E., II (1994) *Biochemistry 33*, 4291−4299.
Greenfield, N., & Fasman, G. D. (1969) *Biochemistry 8*, 4108−4116.
Gruner, S. M. (1989) *J. Phys. Chem. 93*, 7562−7570.
Haltia, T., & Freire, E. (1995) *Biochim. Biophys. Acta 1241*, 295−322.
Henderson, R., Baldwin, J. M., Ceska, T. A., Zemlin, F., Beckman, E., & Downing, K. H. (1990) *J. Mol. Biol. 213*, 899−929.
Killian, J. A. (1992) *Biochim. Biophys. Acta 1113*, 391−425.
Killian, J. A., Timmermans, J. W., Keur, S., & De Kruijff, B. (1985) *Biochim. Biophys. Acta 820*, 154−156.
Killian, J. A., Prasad, K. U., Urry, D. W., & De Kruijff, B. (1989) *Biochim. Biophys. Acta 978*, 341−345.
Killian, J. A., Trouard, T. P., Greathouse, D. V., Chupin, V., & Lindblom, G. (1994) *FEBS Lett. 348*, 161−165.
Landolt-Marticorena, C., Williams, K. A., Deber, C. M., & Reithmeier, R. A. F. (1993) *J. Mol. Biol. 229*, 602−608.
Lindblom, G., & Rilfors, L. (1989) *Biochim. Biophys. Acta 988*, 221−256.
Lindblom, G., & Rilfors, L. (1992) in *Structural and Dynamic Properties of Lipids and Membranes* (Quinn, P. J., & Cherry, R. J., Eds.) pp 51−76, Portland Press, London.
Lindblom, G., Lindman, B., & Mandell, L. (1973) *J. Colloid Interface Sci. 42*, 400−409.
Lewis, B. A., & Engelman, D. M. (1983a) *J. Mol. Biol. 166*, 203−210.
Lewis, B. A., & Engelman, D. M. (1983b) *J. Mol. Biol. 166*, 211−217.
Marsh, D. (1995) *Mol. Membr. Biol. 12*, 59−64.
Michel, H., & Deisenhofer, J. (1990) *Curr. Top. Membr. Transp. 36*, 53−69.
Montecucco, C., Smith, G. A., Dabbeni-sala, F., Johansson, A., Galante, Y. M., & Bisson, R. (1982) *FEBS Lett. 144*, 145−148.
Mouritsen, O. G., & Bloom, M. (1984) *Biophys. J. 46*, 141−153.
O'Connell, A. M., Koeppe, R. E., & Andersen, O. S. (1990) *Science 250*, 1256−1259.
Pauls, K. P., MacKay, A. L., Soderman, O., Bloom, M., Tanjea, A. K., & Hodges, R. S. (1985) *Eur. Biophys. J. 12*, 1−11.
Pelham, H. R., & Munro, S. (1993) *Cell 75*, 603−605.
Piknova, B., Perochon, E., & Tocanne, J.-F. (1993) *Eur. J. Biochem. 218*, 385−396.
Riegler, J., & Möhwald, H. (1986) *Biophys. J. 49*, 1111−1118.
Rouser, G., Fleischer, S., & Yamamota, A. (1970) *Lipids 5*, 494−496.
Roux, M. R., Neumann, J. M., Hodges, R. S., Devaux, P. F., & Bloom, M. (1989) *Biochemistry 28*, 2313−2321.
Salom, D., Baño, M. C., & Abad, C. (1995) *Biochem. Biophys. Res. Commun. 209*, 466−473.
Schulz, G. E. (1994) in *Bacterial Cell Wall* issue (Ghuysen, J.-M., & Hakenbeck, R., Eds.) Vol. 27, pp 343−352, Elsevier Series on New Comprehensive Biochemistry, Elsevier, New York.
Seelig, J. (1978) *Biochim. Biophys. Acta 515*, 105−140.
Sjölund, M., Rilfors, L., & Lindblom, G. (1989) *Biochemistry 28*, 1323−1329 .
Sperotto, M. M., & Mouritsen, O. G. (1988) *Eur. Biophys. J. 16*, 1−10.
Sperotto, M. M., & Mouritsen, O. G. (1993) *Eur. Biophys. J. 22*, 323−328.
Urry, D. W., Goodall, M. C., Glickson, J. D., & Mayers, D. F. (1971) *Proc. Natl. Acad. Sci. U.S.A. 68*, 1907−1911.
Van Dijck, P. W. M., De Kruijff, B., Van Deenen, L. L. M., De Gier, J., & Demel, R. A. (1976) *Biochim. Biophys. Acta 455*, 576−587.
Van Echteld, C. J. A., De Kruijff, B., Verkleij, A. J., Leunissen-Bijvelt, J., & De Gier, J. (1982) *Biochim. Biophys. Acta 692*, 126−138.
Watnick, P. I., Chan, S. I., & Dea, P. (1990) *Biochemistry 29*, 6215−6221.
Weiss, L. B., & Koeppe, R. E., II (1985) *Int. J. Protein Pept. Res. 26*, 305−310.
Weiss, M. S., Abele, U., Weckesser, J., Welte, W., Schiltz, E., & Schultz, G. E. (1991) *Science 254*, 1627−1630.
White, S. H., & Wimley, W. C. (1994) *Curr. Opin. Struct. Biol. 4*, 79−86.
Wimley, W. C., & White, S. (1993) *Biochemistry 32*, 6307−6312.
Xing, J., & Scott, H. L. (1992) *Biochim. Biophys. Acta 1106*, 227−232.
Zhang, Y.-P., Lewis, R. N. A. H., Hodges, R. S., & McElhaney, R. N. (1992) *Biochemistry 31*, 11579−11588.
Zhang, Y.-P., Lewis, R. N. A. H., Henry, G. D., Sykes, B., Hodges, R. S., & McElhaney, R. N. (1995a) *Biochemistry 34*, 2348−2361.
Zhang, Y.-P., Lewis, R. N. A. H., Hodges, R. S., & McElhaney, R. N. (1995b) *Biochemistry 34*, 2362−2371.

BI9519258